Double-beta decay nuclear matrix elements: the theoretical challenge

Nunzio Itaco

Università della Campania “Luigi Vanvitelli”
Istituto Nazionale di Fisica Nucleare - Sezione di Napoli

Marciana 2023
Lepton Interactions with Nucleons and Nuclei

Università degli Studi della Campania *Luigi Vanvitelli*

INFN Istituto Nazionale di Fisica Nucleare

Double β-decay

Double β-decay (2νECEC) is the rarest process yet observed in nature.

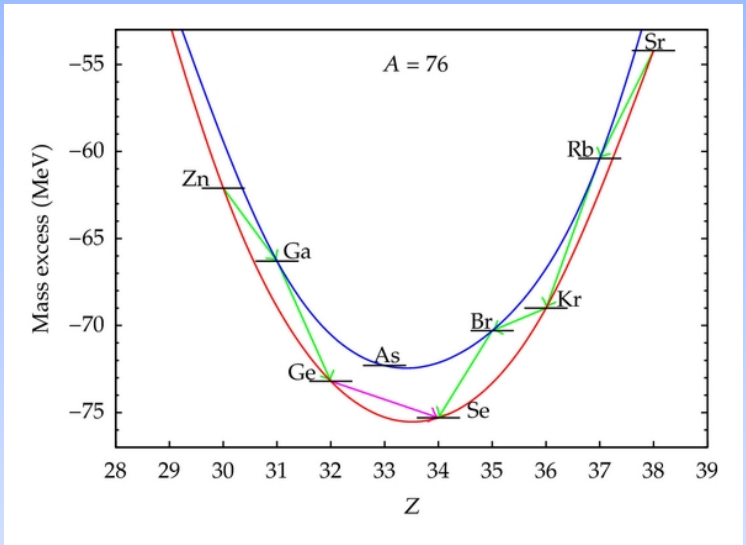

- Maria Goeppert-Mayer (1935) suggested the possibility to detect
  $(A, Z) \rightarrow (A, Z+2) + e^- + e^- + \overline{\nu}_e + \overline{\nu}_e$

- Historically, G. Racah (1937) and W. Furry (1939) were the first ones, to suggest to test the neutrino as a Majorana particle, considering the process:
  $(A, Z) \rightarrow (A, Z+2) + e^- + e^-$

Double β-decay

Double β-decay (2νECEC) is the rarest process yet observed in nature.

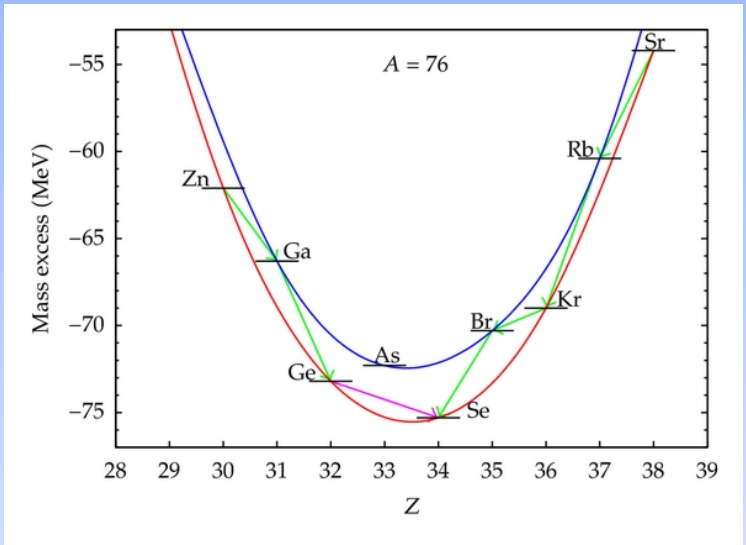

- Maria Goeppert-Mayer (1935) suggested the possibility to detect
  $(A, Z) \rightarrow (A, Z+2) + e^- + e^- + \overline{\nu}_e + \overline{\nu}_e$
- Historically, G. Racah (1937) and W. Furry (1939) were the first ones, to suggest to test the neutrino as a Majorana particle, considering the process:
  $(A, Z) \rightarrow (A, Z+2) + e^- + e^-$

Double β-decay

Double β-decay (2νECEC) is the rarest process yet observed in nature.

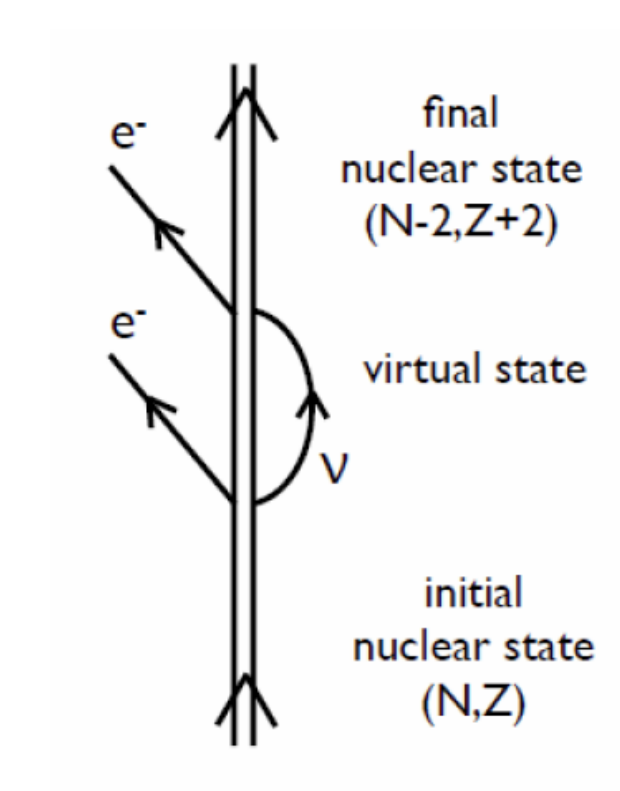

- Maria Goeppert-Mayer (1935) suggested the possibility to detect
  $(A, Z) \rightarrow (A, Z+2) + e^- + e^- + \overline{\nu}_e + \overline{\nu}_e$
- Historically, G. Racah (1937) and W. Furry (1939) were the first ones, to suggest to test the neutrino as a Majorana particle, considering the process:
  $(A, Z) \rightarrow (A, Z+2) + e^- + e^-$

Neutrinoless double β-decay

The detection of the $0\nu\beta\beta$ decay is nowadays one of the main targets in many laboratories all around the world, triggered by the search of "new physics" beyond the Standard Model.

- Its detection
  - $\Rightarrow$ violation of the conservation of the leptonic number
  - $\Rightarrow$ more informations on the nature of neutrinos (neutrino as a Majorana particle, determination of its effective mass, ..).
  - $\Rightarrow$ creation of matter without antimatter, which has never been observed (since the Big Bang)
    $(A, Z) \rightarrow (A, Z+2) + e^- + e^-$

Neutrinoless double β-decay

The inverse of the $0\nu\beta\beta$-decay half-life is proportional to the squared nuclear matrix element (NME).
This evidences the relevance to calculate the NME

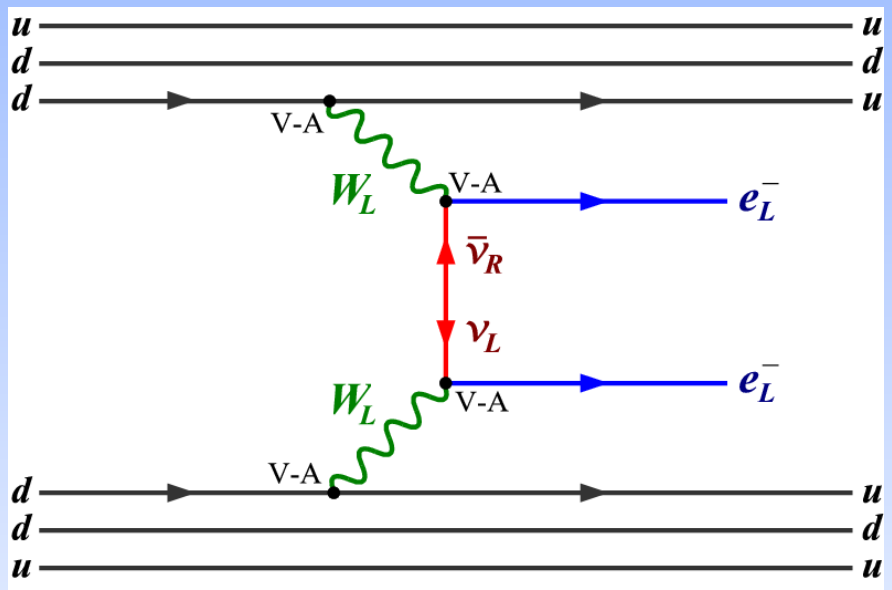

$$\left[T_{1/2}^{0\nu}\right]^{-1} = G^{0\nu}\left|M^{0\nu}\right|^2\left|\frac{m_{\beta\beta}}{m_e}\right|^2$$

light neutrino exchange

- $G^{0\nu} \rightarrow$ phase-space factor
- $m_{\beta\beta} = |\sum_k m_k U_{ek}^2|$ effective mass of the Majorana neutrino, U_{ek} being the lepton mixing matrix

Neutrinoless double β-decay

The inverse of the $0\nu\beta\beta$-decay half-life is proportional to the squared nuclear matrix element (NME).
This evidences the relevance to calculate the NME

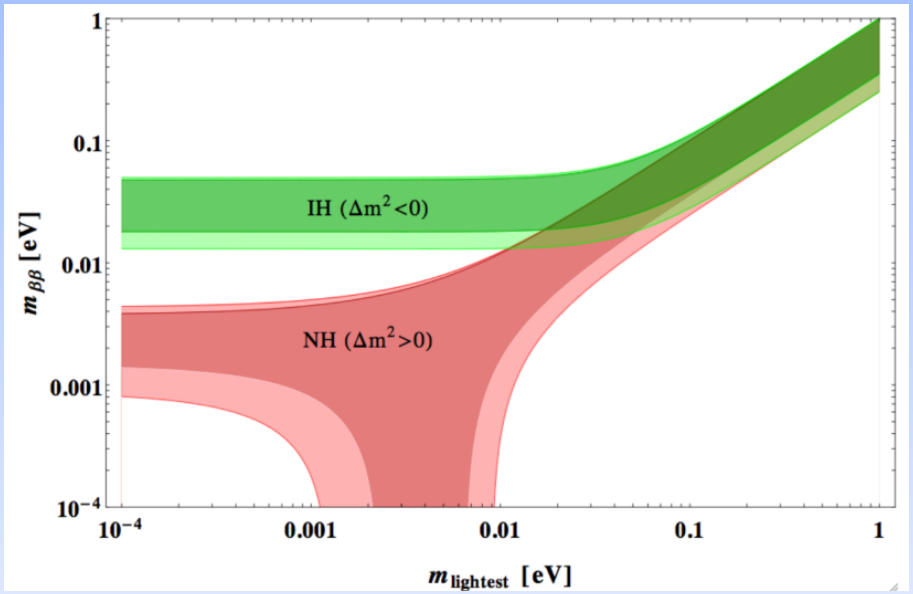

$$\left[T^{0\nu}_{1/2}\right]^{-1} = G^{0\nu}\left|M^{0\nu}\right|^2\left|\frac{m_{\beta\beta}}{m_e}\right|^2$$

light neutrino exchange

- constraints from oscillation data
- smallest allowed $m_{\beta\beta}$ value for IH $\Rightarrow 18.4 \pm 1.3$ meV

Neutrinoless double β-decay

The inverse of the $0\nu\beta\beta$-decay half-life is proportional to the squared nuclear matrix element (NME).
This evidences the relevance to calculate the NME

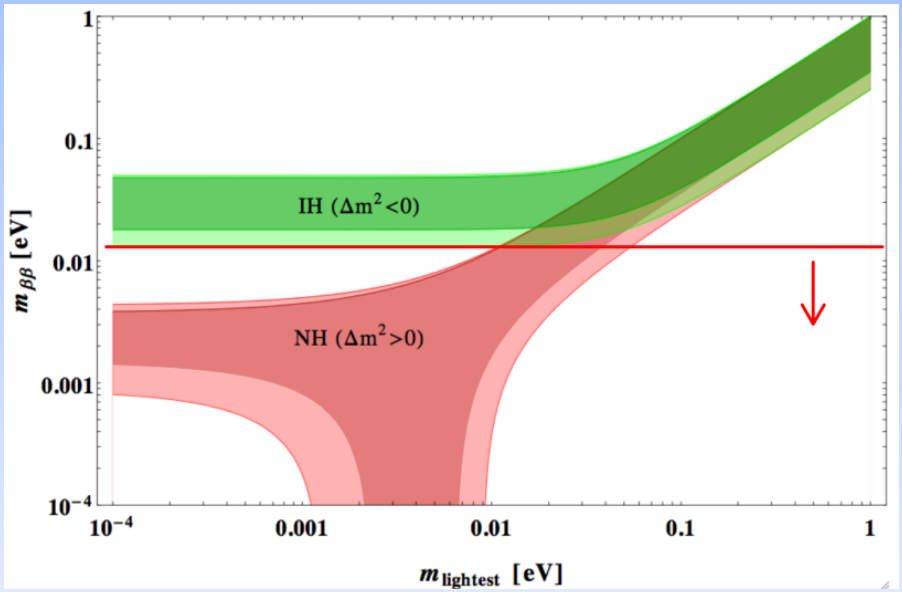

$$\left[T^{0\nu}_{1/2}\right]^{-1} = G^{0\nu}\left|M^{0\nu}\right|^2\left|\frac{m_{\beta\beta}}{m_e}\right|^2$$

light neutrino exchange

- constraints from oscillation data
- smallest allowed $m_{\beta\beta}$ value for IH $\Rightarrow 18.4 \pm 1.3$ meV

The calculation of the NME

The nuclear matrix element (NME) is expressed as

$$M^{0\nu} = M^{0\nu}_{GT} - \left(\frac{g_V}{g_A}\right)^2 M^{0\nu}_{F} + M^{0\nu}_{T} \ ,$$

where (*light neutrino exchange*)

$$M^{0\nu}_{GT} = < 0^+_f \mid \sum_{m,n} \tau^-_m \tau^-_n H_{GT}(r_{mn}) \vec{\sigma}_m \cdot \vec{\sigma}_n \mid 0^+_i >$$

$$M^{0\nu}_{F} = < 0^+_f \mid \sum_{m,n} \tau^-_m \tau^-_n H_{F}(r_{mn}) \mid 0^+_i >$$

$$M^{0\nu}_{T} = < 0^+_f \mid \sum_{m,n} \tau^-_m \tau^-_n H_{T}(r_{mn}) \left[3 \left(\vec{\sigma}_m \cdot \hat{r}_{mn}\right) \left(\vec{\sigma}_n \cdot \hat{r}_{mn}\right) - \vec{\sigma}_m \cdot \vec{\sigma}_n\right] \mid 0^+_i >$$

The calculation of the NME

To describe the nuclear properties detected in the experiments, one needs to resort to nuclear structure models.

Mean-field and collective models

- Energy Density Functional (EDF)
- Quasiparticle Random-Phase Approximation (QRPA)
- Interacting Boson Model IBM

Microscopic approaches

- *Ab initio* methods
  - No-Core Shell Model (NCSM)
  - Coupled-Cluster Method (CCM)
  - In-Medium Similarity Renormalization Group (IMSRG)
  - Self-Consistent Green's Function approach (SCGF)
- Nuclear Shell Model

The calculation of the NME

To describe the nuclear properties detected in the experiments, one needs to resort to nuclear structure models.

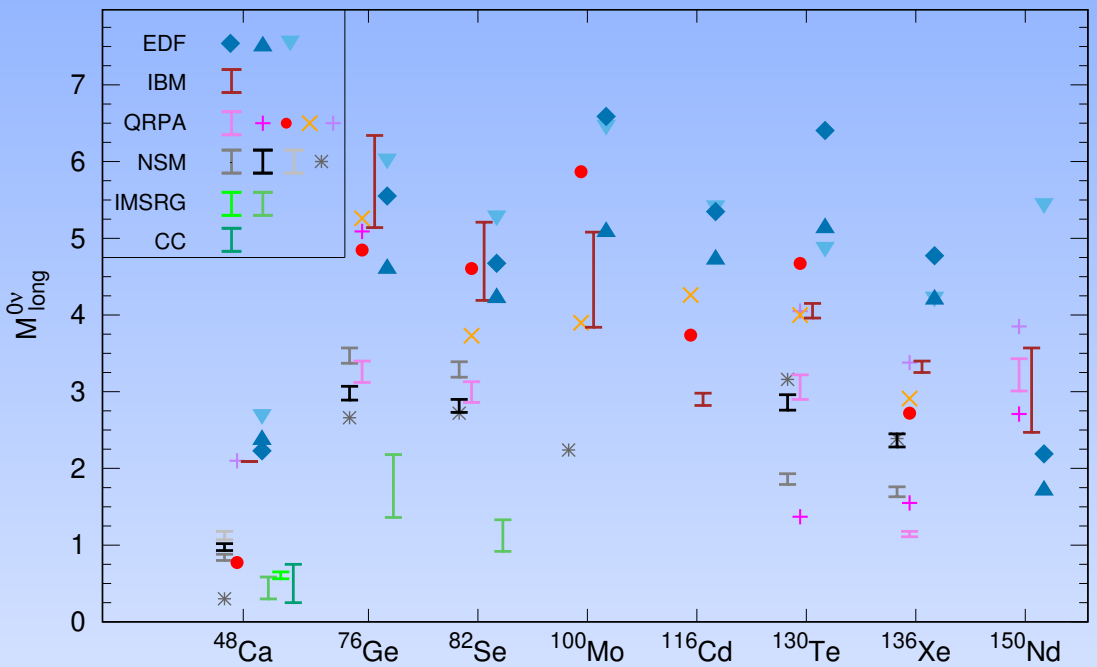

M. Agostini, G. Benato, J. Detwiler, J. Menendez, F. Vissani, Rev. Mod. Phys. 95, 025002 (2023)

- The spread of nuclear structure calculations evidences inconsistencies among results obtained with different models

Realistic Shell-Model Calculations

Shell model $\Rightarrow$ well-established approach to obtain a microscopic description of both collective and single-particle properties of nuclei

Università "Vanvitelli" and INFN-Napoli
- L. Coraggio
- G. De Gregorio
- A. Gargano
- N. I.

INFN-Pisa
- M. Viviani

Peking University
- Z. H. Cheng
- Y. Z. Ma
- F. R. Xu

IPHC-CNRS Strasbourg
- F. Nowacki

GSI Darmstadt
- R. Mancino

Università degli Studi della Campania *Luigi Vanvitelli*

INFN Istituto Nazionale di Fisica Nucleare

Realistic Shell-Model Calculations

Focus on ^{76}Ge, ^{82}Se, ^{100}Mo, ^{130}Te, and ^{136}Xe.

^{76}Ge

- GERDA-II
- MJD
- LEGEND-200
- LEGEND-1000

^{82}Se

- CUPID-0
- SuperNEMO-D
- SuperNEMO

^{136}Xe

- EXO-200
- nEXO
- NEXT-100
- NEXT-HD
- PandaX-III
- LZ-nat
- LZ-enr
- DARWIN
- KLZ-400
- KLZ-800
- KL2Z

^{100}Mo

- CUPID-Mo
- CUPID
- CROSS
- Amore-II
- NEMO-3

^{130}Te

- SNO+
- SNO+II
- CUORE

Realistic Shell-Model Calculations

Shell model $\Rightarrow$ well-established approach to obtain a microscopic description of both collective and single-particle properties of nuclei

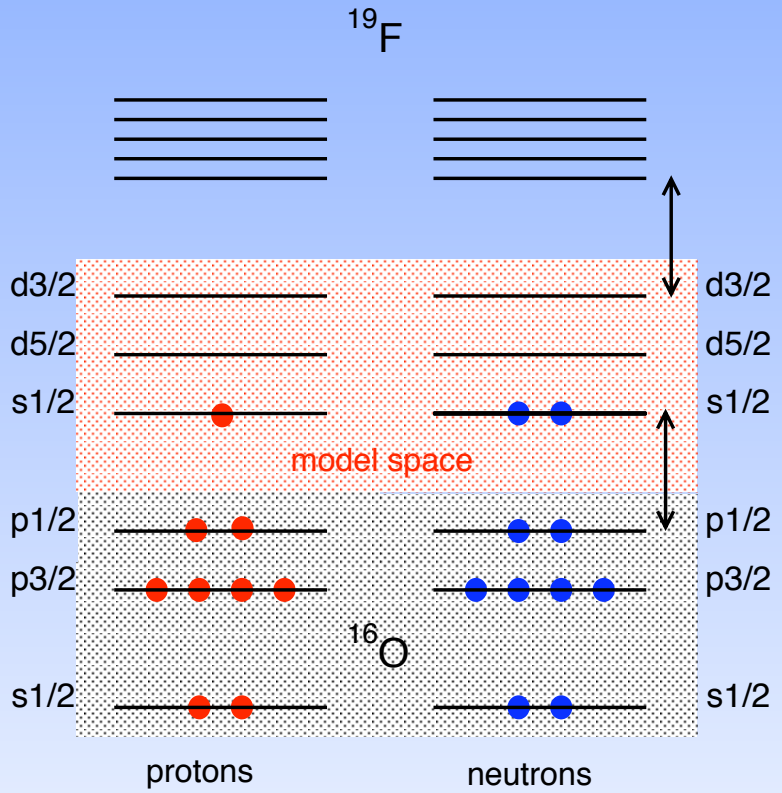

The degrees of freedom of the core nucleons and the excitations of the valence ones above the model space are not considered explicitly.

$$V_{NN} \ (+V_{NNN}) \Rightarrow \text{many-body theory} \Rightarrow H_{\text{eff}}$$

Effective shell-model hamiltonian

A-nucleon system Schrödinger equation

$$H|\Psi_\nu\rangle = E_\nu|\Psi_\nu\rangle$$

$$H = H_0 + H_1 = \sum_{i=1}^{A}(T_i + U_i) + \sum_{i<j}(V_{ij}^{NN} - U_i)$$

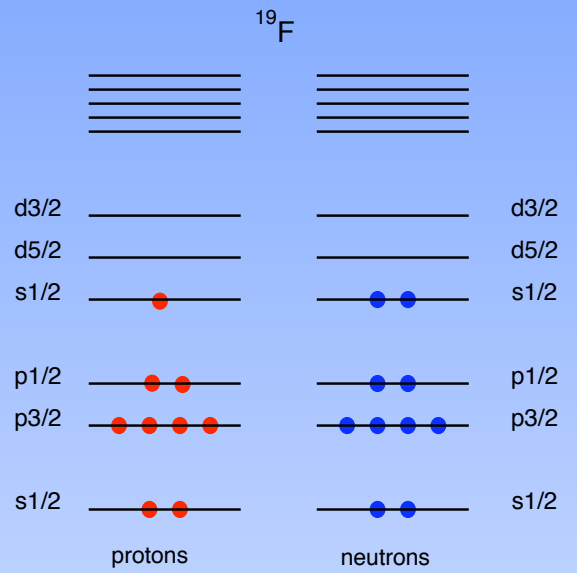

Effective shell-model hamiltonian

A-nucleon system Schrödinger equation

$$H|\Psi_\nu\rangle = E_\nu|\Psi_\nu\rangle$$

$$H = H_0 + H_1 = \sum_{i=1}^{A}(T_i + U_i) + \sum_{i<j}(V_{ij}^{NN} - U_i)$$

Model space

$$|\Phi_i\rangle = [a_1^\dagger a_2^\dagger \ldots a_n^\dagger]_i|c\rangle \Rightarrow P = \sum_{i=1}^{d}|\Phi_i\rangle\langle\Phi_i|$$

Model-space eigenvalue problem

$$H_{\rm eff}P|\Psi_\alpha\rangle = E_\alpha P|\Psi_\alpha\rangle$$

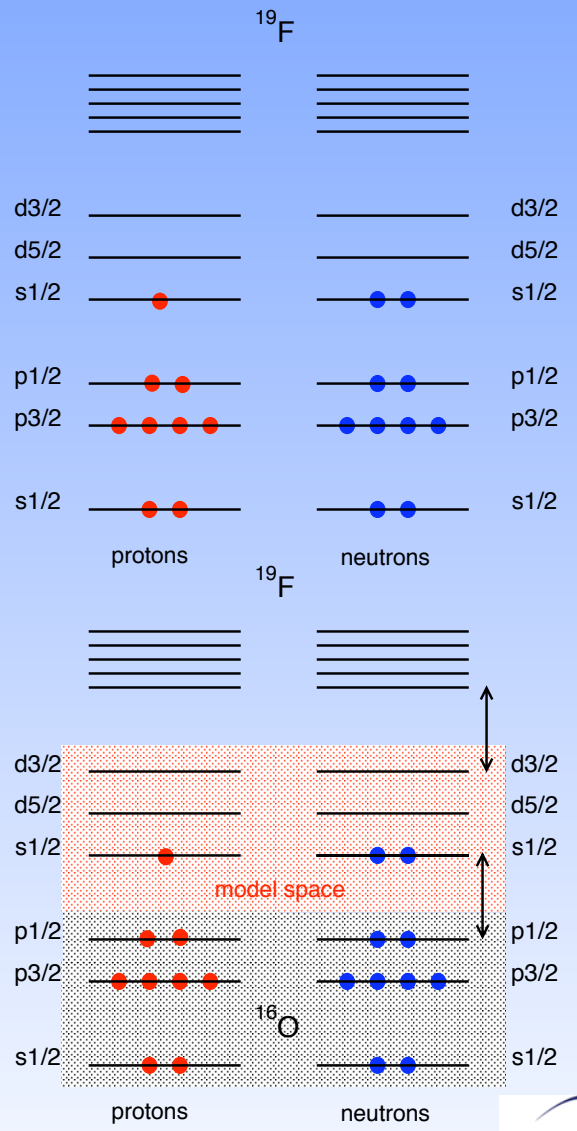

Effective shell-model Hamiltonian

$$\left(\begin{array}{c|c} PHP & PHQ \\ \hline QHP & QHQ \end{array}\right) \quad \mathcal{H} = \Omega^{-1} H \Omega \quad \Longrightarrow \quad \left(\begin{array}{c|c} P\mathcal{H}P & P\mathcal{H}Q \\ \hline 0 & Q\mathcal{H}Q \end{array}\right)$$

$$Q\mathcal{H}P = 0$$

$$H_{\text{eff}} = P\mathcal{H}P$$

$$\text{Suzuki \& Lee} \Rightarrow \Omega = e^{\omega} \text{ with } \omega = \left(\begin{array}{c|c} 0 & 0 \\ \hline Q\omega P & 0 \end{array}\right)$$

$$H_1^{\text{eff}}(\omega) = PH_1P + PH_1Q\frac{1}{\epsilon - QHQ}QH_1P - PH_1Q\frac{1}{\epsilon - QHQ}\omega H_1^{\text{eff}}(\omega)$$

The shell-model effective hamiltonian

Folded-diagram expansion

$\hat{Q}$-box vertex function

$$\hat{Q}(\epsilon) = PH_1P + PH_1Q\frac{1}{\epsilon - QHQ}QH_1P$$

$\Rightarrow$ Recursive equation for $H_{\text{eff}} \Rightarrow$ iterative techniques (Krenciglowa-Kuo, Lee-Suzuki, ...)

$$H_{\text{eff}} = \hat{Q} - \hat{Q}' \int \hat{Q} + \hat{Q}' \int \hat{Q} \int \hat{Q} - \hat{Q}' \int \hat{Q} \int \hat{Q} \int \hat{Q} \cdots ,$$

generalized folding

The perturbative approach to the shell-model H^{eff}

$$\hat{Q}(\epsilon) = PH_1P + PH_1Q\frac{1}{\epsilon - QHQ}QH_1P$$

The $\hat{Q}$-box can be calculated perturbatively

$$\frac{1}{\epsilon - QHQ} = \sum_{n=0}^{\infty} \frac{(QH_1Q)^n}{(\epsilon - QH_0Q)^{n+1}}$$

The diagrammatic expansion of the $\hat{Q}$-box

The perturbative approach to the shell-model H^{eff}

$$\hat{Q}(\epsilon) = PH_1P + PH_1Q\frac{1}{\epsilon - QHQ}QH_1P$$

The $\hat{Q}$-box can be calculated perturbatively

$$\frac{1}{\epsilon - QHQ} = \sum_{n=0}^{\infty} \frac{(QH_1Q)^n}{(\epsilon - QH_0Q)^{n+1}}$$

The diagrammatic expansion of the $\hat{Q}$-box

The perturbative approach to the shell-model H^{eff}

$$\hat{Q}(\epsilon) = PH_1P + PH_1Q\frac{1}{\epsilon - QHQ}QH_1P$$

The $\hat{Q}$-box can be calculated perturbatively

$$\frac{1}{\epsilon - QHQ} = \sum_{n=0}^{\infty} \frac{(QH_1Q)^n}{(\epsilon - QH_0Q)^{n+1}}$$

The diagrammatic expansion of the $\hat{Q}$-box

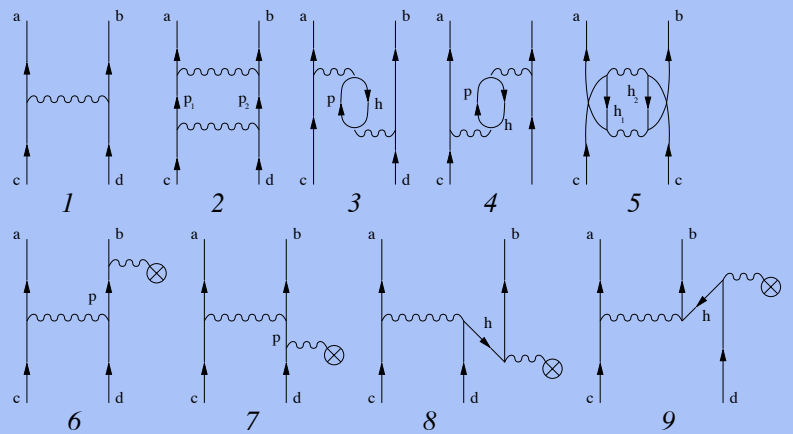

Effective operators

$\Phi_\alpha =$ eigenvectors obtained diagonalizing H_{eff} in the reduced model space $\Rightarrow |\Phi_\alpha\rangle = P|\Psi_\alpha\rangle$

$$\langle\Phi_\alpha|\hat{\Theta}|\Phi_\beta\rangle \neq \langle\Psi_\alpha|\hat{\Theta}|\Psi_\beta\rangle$$

Effective operators

$\Phi_\alpha =$ eigenvectors obtained diagonalizing H_{eff} in the reduced model space $\Rightarrow |\Phi_\alpha\rangle = P|\Psi_\alpha\rangle$

$$\langle\Phi_\alpha|\hat{\Theta}|\Phi_\beta\rangle \neq \langle\Psi_\alpha|\hat{\Theta}|\Psi_\beta\rangle$$

Effective operator $\hat{\Theta}_{\text{eff}}$: definition

$$\hat{\Theta}_{\text{eff}} = \sum_{\alpha\beta} |\Phi_\alpha\rangle\langle\Psi_\alpha|\hat{\Theta}|\Psi_\beta\rangle\langle\Phi_\beta|$$

$$\langle\Phi_\alpha|\hat{\Theta}_{\text{eff}}|\Phi_\beta\rangle = \langle\Psi_\alpha|\hat{\Theta}|\Psi_\beta\rangle$$

Effective operators

$\Phi_\alpha =$ eigenvectors obtained diagonalizing H_{eff} in the reduced model space $\Rightarrow |\Phi_\alpha\rangle = P|\Psi_\alpha\rangle$

$$\langle\Phi_\alpha|\hat{\Theta}|\Phi_\beta\rangle \neq \langle\Psi_\alpha|\hat{\Theta}|\Psi_\beta\rangle$$

Effective operator $\hat{\Theta}_{\text{eff}}$: definition

$$\hat{\Theta}_{\text{eff}} = \sum_{\alpha\beta} |\Phi_\alpha\rangle\langle\Psi_\alpha|\hat{\Theta}|\Psi_\beta\rangle\langle\Phi_\beta|$$

$$\langle\Phi_\alpha|\hat{\Theta}_{\text{eff}}|\Phi_\beta\rangle = \langle\Psi_\alpha|\hat{\Theta}|\Psi_\beta\rangle$$

$\hat{\Theta}_{\text{eff}}$ can be derived consistently in the MBPT framework

K. Suzuki and R. Okamoto, Prog. Theor. Phys. **93** *, 905 (1995)*

The shell-model effective operators

One-body operator

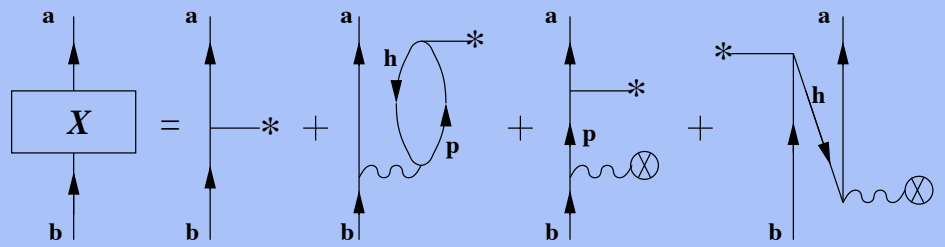

Two-body operator

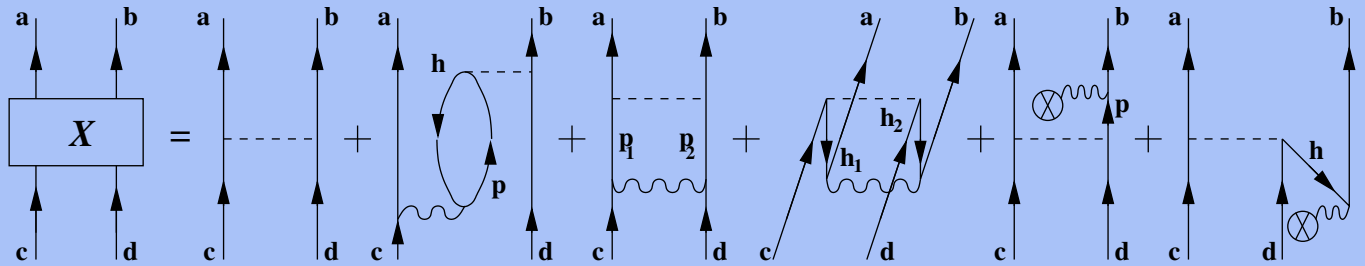

Nuclear models and predictive power

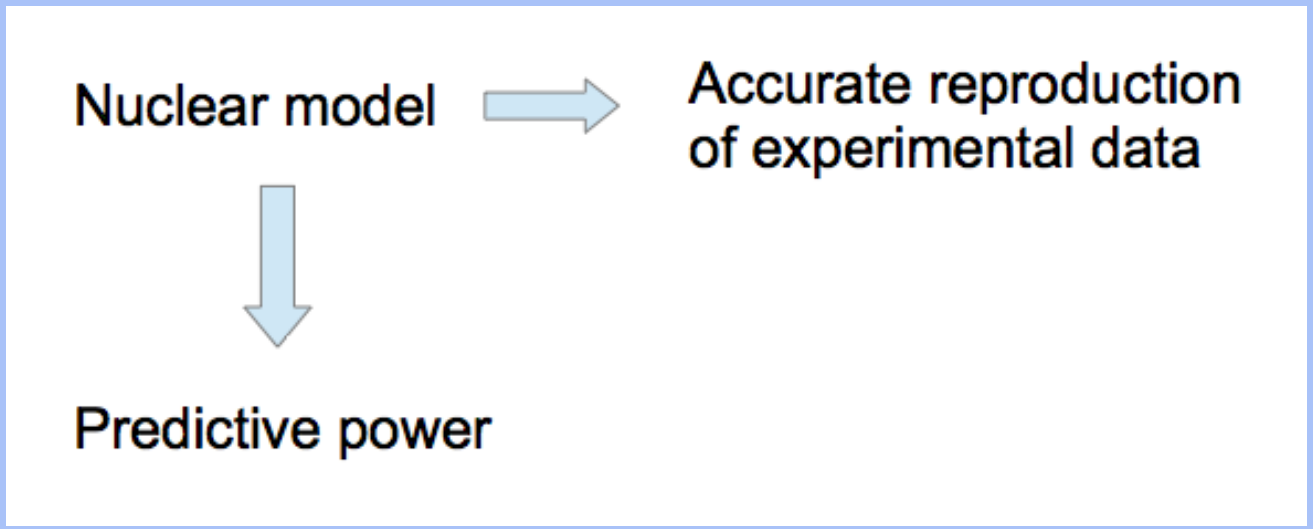

Realistic shell-model calculations for
^{130}Te, ^{136}Xe, ^{100}Mo, ^{76}Ge and ^{82}Se

⇓

Test our approach calculating spectroscopic properties and observables related to the GT strengths and $2\nu\beta\beta$ decay and comparing the results with data.

Realistic Shell-Model Calculations

- ^{76}Ge,^{82}Se: four proton and neutron orbitals outside doubly-closed ^{56}Ni $\rightarrow$ $0f_{5/2}, 1p_{3/2}, 1p_{1/2}, 0g_{9/2}$
- ^{100}Mo: four proton $\rightarrow$ $\pi 0f_{5/2}, 1p_{3/2}, 1p_{1/2}, 0g_{9/2}$ and four neutron orbitals $\rightarrow$ $0g_{7/2}, 1d_{5/2}, 1d_{3/2}, 2s_{1/2}$ outside doubly-closed ^{78}Ni
- ^{130}Te,^{136}Xe: five proton and neutron orbitals outside doubly-closed ^{100}Sn $\rightarrow$ $0g_{7/2}, 1d_{5/2}, 1d_{3/2}, 2s_{1/2}, 0h_{11/2}$

Realistic Shell-Model Calculations

- ^{76}Ge,^{82}Se: four proton and neutron orbitals outside doubly-closed ^{56}Ni $\rightarrow$ $0f_{5/2}, 1p_{3/2}, 1p_{1/2}, 0g_{9/2}$
- ^{100}Mo: four proton $\rightarrow$ $\pi 0f_{5/2}, 1p_{3/2}, 1p_{1/2}, 0g_{9/2}$ and four neutron orbitals $\rightarrow$ $0g_{7/2}, 1d_{5/2}, 1d_{3/2}, 2s_{1/2}$ outside doubly-closed ^{78}Ni
- ^{130}Te,^{136}Xe: five proton and neutron orbitals outside doubly-closed ^{100}Sn $\rightarrow$ $0g_{7/2}, 1d_{5/2}, 1d_{3/2}, 2s_{1/2}, 0h_{11/2}$

- Input V_{NN}: $V_{\mathrm{low-k}}$ derived from the high-precision *NN* CD-Bonn potential with a cutoff: $\Lambda = 2.6$ fm^{-1}.
- H_{eff} obtained calculating the Q-box up to the 3rd order in $V_{\mathrm{low-k}}$
- Effective operators are consistently derived by way of the MBPT

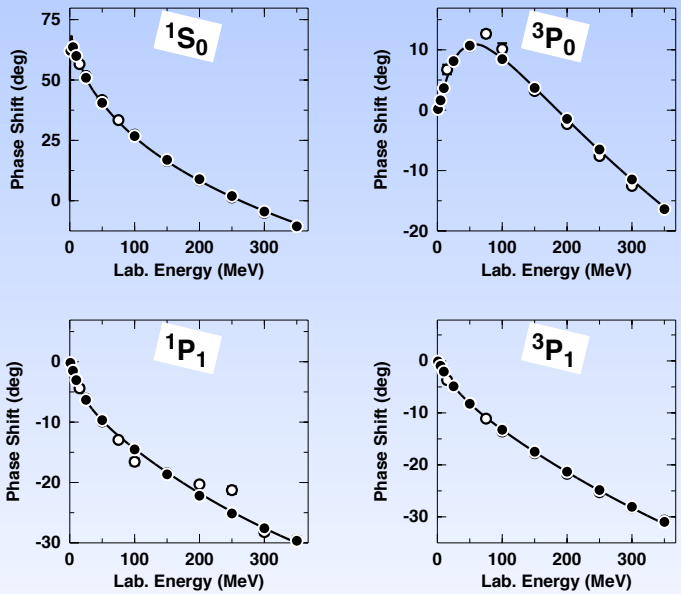

Spectroscopic properties (B(E2)s in e^2fm^4)

$^{76}Ge \rightarrow {}^{76}Se$

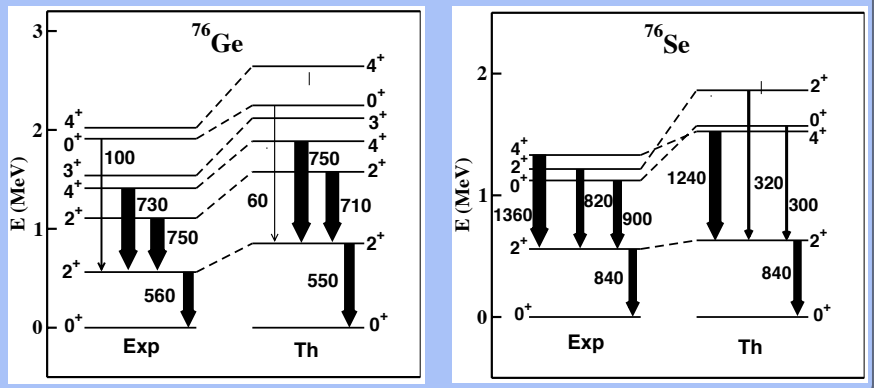

$^{82}Se \rightarrow {}^{82}Kr$

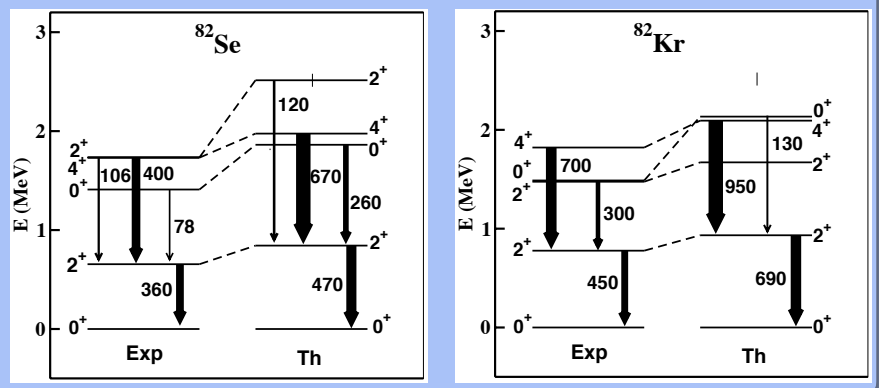

$^{130}Te \rightarrow {}^{130}Xe$

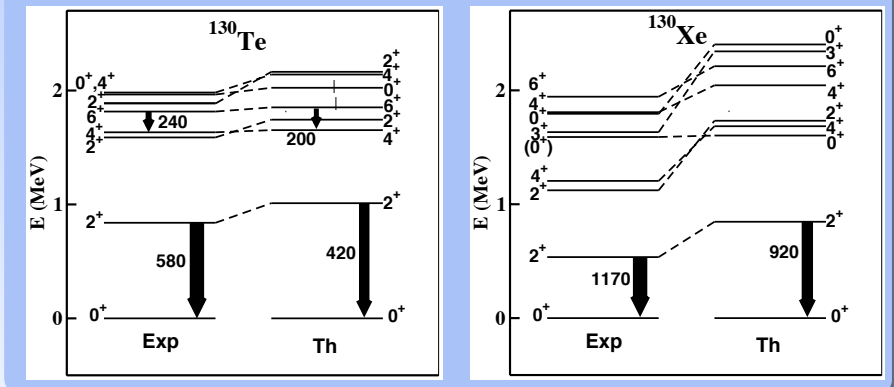

$^{136}Xe \rightarrow {}^{136}Ba$

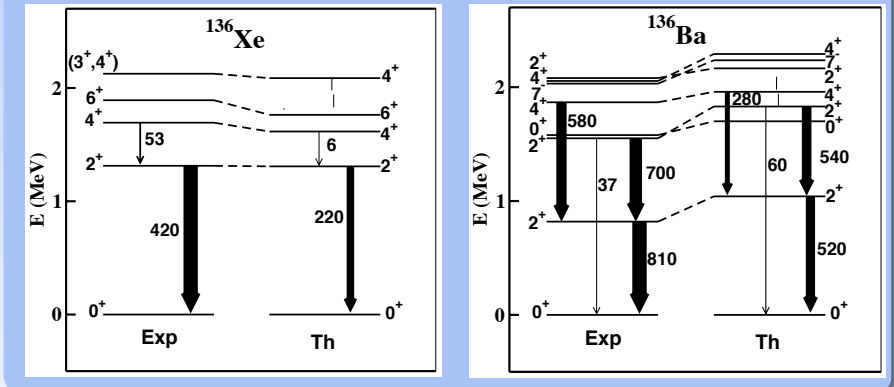

Spectroscopic properties (B(E2)s in e^2fm^4)

$^{100}Mo \rightarrow {}^{100}Ru$

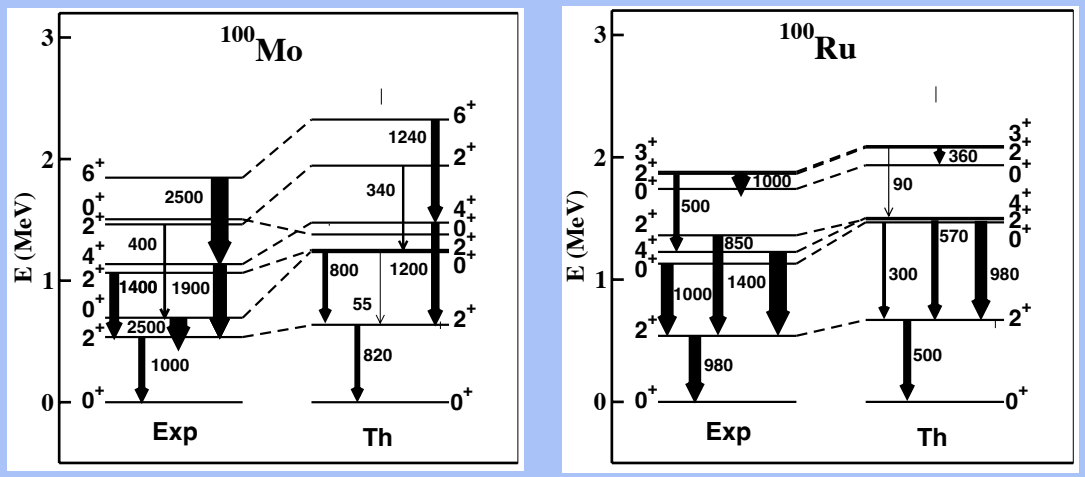

First shell-model calculation of ^{100}Mo decay

L. Coraggio, NI., G. De Gregorio, A. Gargano, R. Mancino, and F. Nowacki, Phys. Rev. C **105** *034312 (2022)*

GT strength distributions

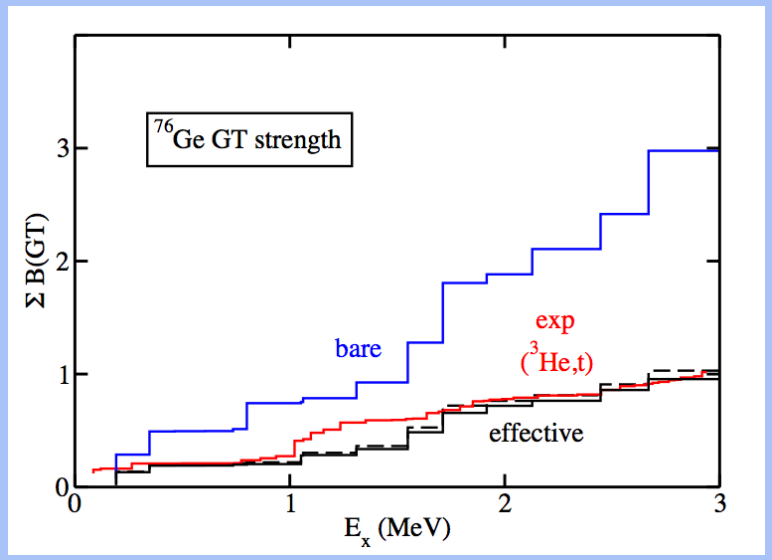

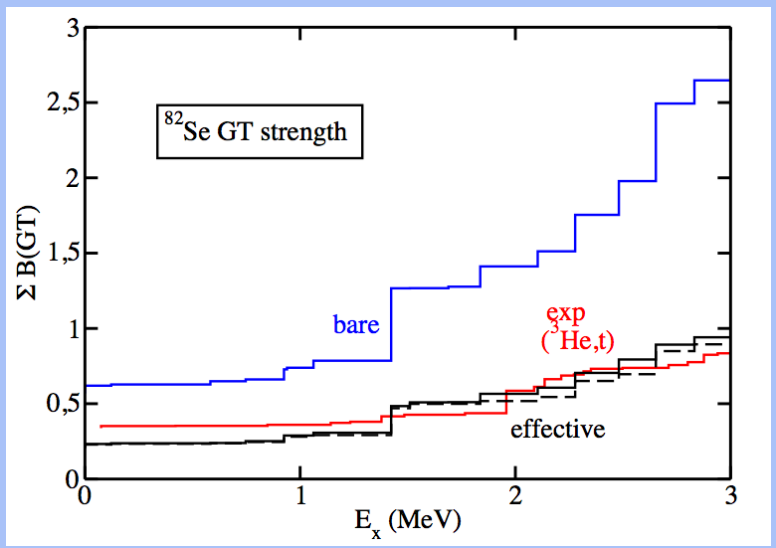

Charge-exchange experiments

$$\left[\frac{d\sigma}{d\Omega}(q=0)\right] = \hat{\sigma} B_{exp}(GT)$$

$$B_{Th}(GT) = \frac{|\langle \Phi_f || \boldsymbol{\sigma}\boldsymbol{\tau}^{\pm} || \Phi_i \rangle|^2}{2J_i + 1}$$

GT strength distributions

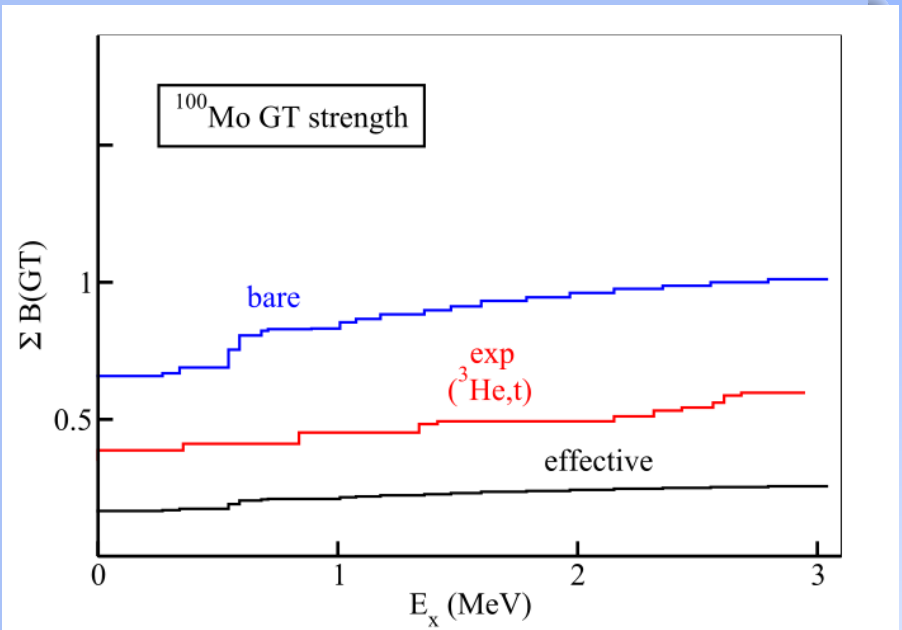

Charge-exchange experiments

$$\left[\frac{d\sigma}{d\Omega}(q=0)\right] = \hat{\sigma} B_{exp}(GT)$$

$$B_{Th}(GT) = \frac{|\langle \Phi_f || \boldsymbol{\sigma}\boldsymbol{\tau}^{\pm} || \Phi_i \rangle|^2}{2J_i + 1}$$

GT strength distributions

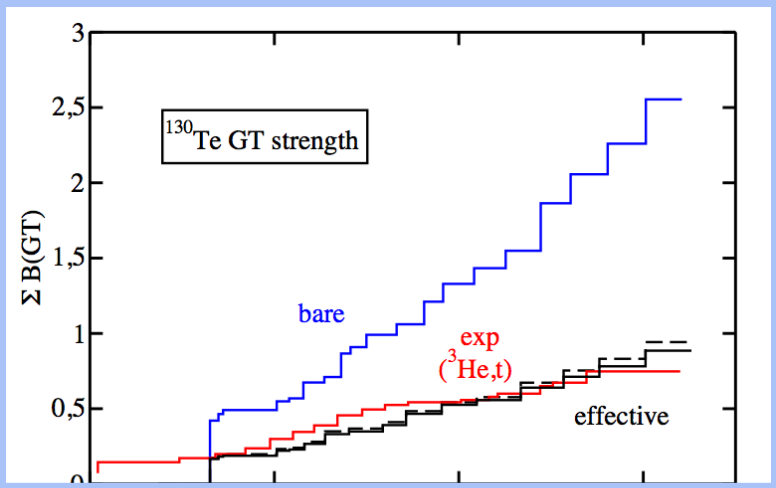

Charge-exchange experiments

$$\left[\frac{d\sigma}{d\Omega}(q=0)\right] = \hat{\sigma} B_{exp}(GT)$$

$$B_{Th}(GT) = \frac{|\langle \Phi_f || \boldsymbol{\sigma}\boldsymbol{\tau}^{\pm} || \Phi_i \rangle|^2}{2J_i + 1}$$

$2\nu\beta\beta$ nuclear matrix elements

$$M_{2\nu}^{\mathrm{GT}} = \sum_n \frac{\langle 0_f^+ || \vec{\sigma}\tau^- || 1_n^+ \rangle \langle 1_n^+ || \vec{\sigma}\tau^- || 0_i^+ \rangle}{E_n + E_0}$$

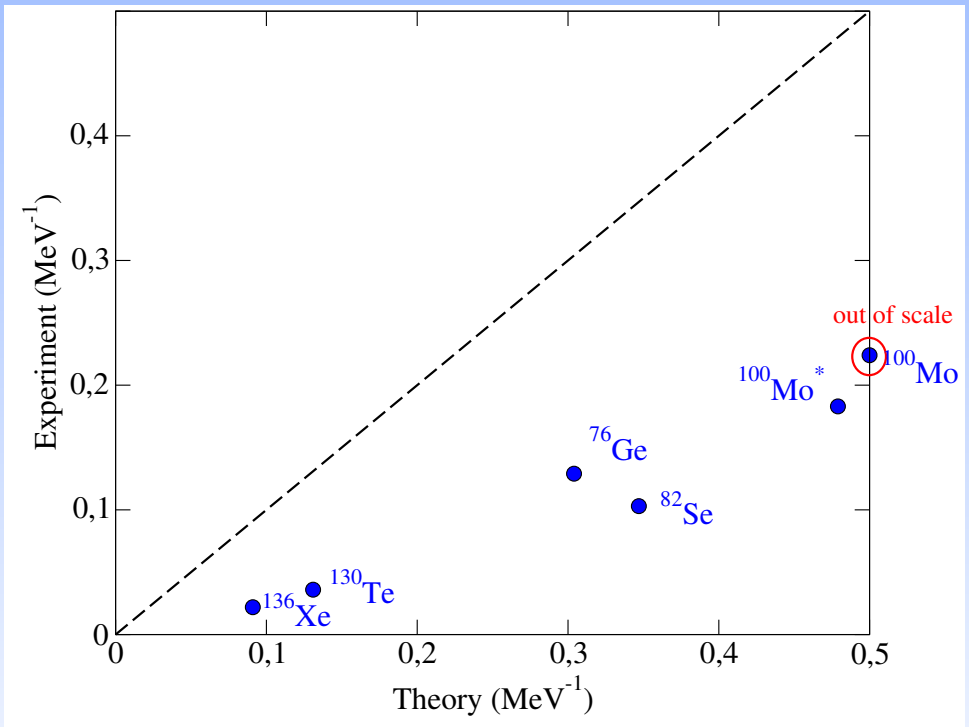

Lanczos strength-function method

Blue dots: bare GT operator

Black triangles: effective GT operator

$2\nu\beta\beta$ nuclear matrix elements

$$M_{2\nu}^{\mathrm{GT}} = \sum_n \frac{\langle 0_f^+ || \vec{\sigma}\tau^- || 1_n^+ \rangle \langle 1_n^+ || \vec{\sigma}\tau^- || 0_i^+ \rangle}{E_n + E_0}$$

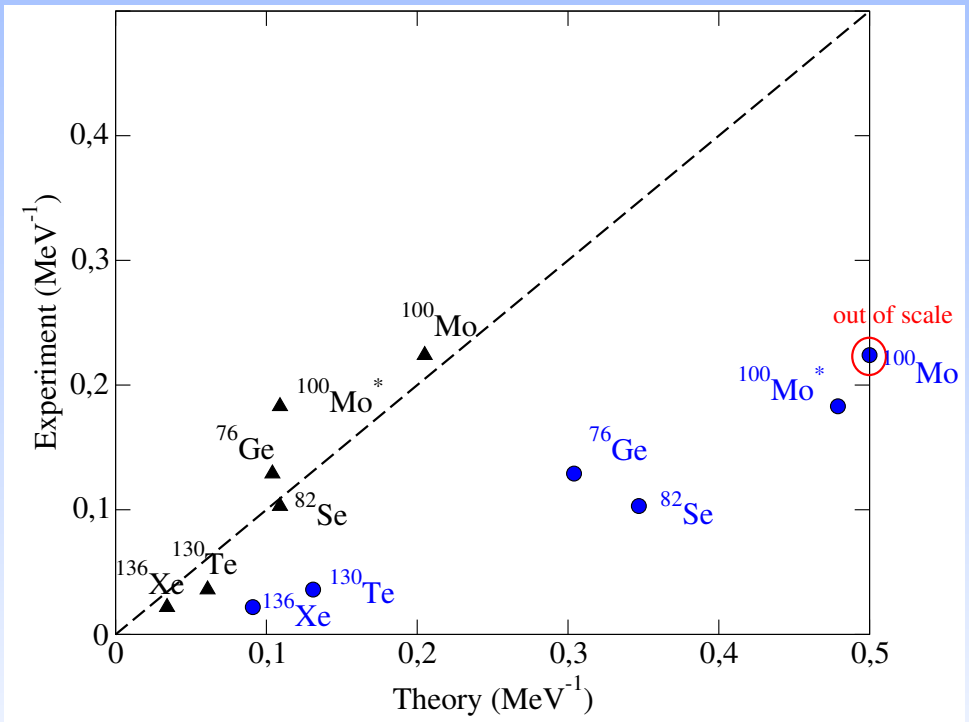

Lanczos strength-function method

Blue dots: bare GT operator
Black triangles: effective GT operator

The calculation of the $0\nu\beta\beta$ NME

The NME is given by

$$M^{0\nu} = M^{0\nu}_{GT} - \left(\frac{g_V}{g_A}\right)^2 M^{0\nu}_{F} + M^{0\nu}_{T} \quad ,$$

The matrix elements $M^{0\nu}_{\alpha}$ are defined, for a SM calculation, as follows:

$$M^{0\nu}_{\alpha} = \sum_{j_p j_{p'} j_n j_{n'} J_\pi} TBTD\left(j_p j_{p'}, j_n j_{n'}; J_\pi\right) \left\langle j_p j_{p'}; J^\pi T \mid \tau_1^- \tau_2^- O^{\alpha}_{12} \mid j_n j_{n'}; J^\pi T \right\rangle$$

with $\alpha = (GT,\ F,\ T)$

The *TBTD* are the two-body transition-density matrix elements, and the Gamow-Teller (GT), Fermi (F), and tensor (T) operators:

$$O^{GT}_{12} = \vec{\sigma}_1 \cdot \vec{\sigma}_2 H_{GT}(r)$$
$$O^{F}_{12} = H_F(r)$$
$$O^{T}_{12} = \left[3\left(\vec{\sigma}_1 \cdot \hat{r}\right)\left(\vec{\sigma}_1 \cdot \hat{r}\right) - \vec{\sigma}_1 \cdot \vec{\sigma}_2\right] H_T(r)$$

Light Majorana neutrino exchange

The neutrino potentials H_α are defined using the closure approximation

$$H_\alpha(r) = \frac{2R}{\pi} \int_0^\infty f_\alpha(qr) \frac{h_\alpha(q^2)}{q + \langle E \rangle} q dq$$

where $f_{F,GT}(qr) = j_0(qr)$ and $f_T(qr) = j_2(qr)$, $\langle E \rangle$ is the average energy used in the closure approximation.

- closure approximation
- higher order corrections (HOC)
- finite nucleon size corrections (FNS)

Short-range correlations

Empirical approach

$$\psi_{nl} \rightarrow [1 + f(r)]\, \psi_{nl} \qquad f(r) = -ce^{-ar^2}(1 - br^2)$$

Short-range correlations

Empirical approach

$$\psi_{nl} \to [1 + f(r)]\, \psi_{nl} \qquad f(r) = -ce^{-ar^2}(1 - br^2)$$

$V_{\mathrm{low-k}}$: the configurations of $V_{NN}(k, k')$ are restricted to those with $k, k' < k_{\mathrm{cutoff}} = \Lambda$

$$V_{NN}(k, k') \to V_{\mathrm{low-k}}(k, k') = \Omega^{-1} V_{NN}(k, k')\Omega$$

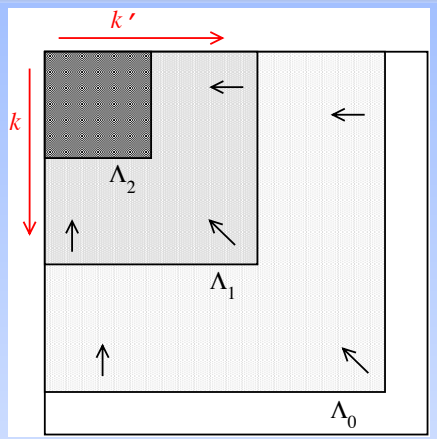

Short-range correlations

Empirical approach

$$\psi_{nl} \to [1 + f(r)]\, \psi_{nl} \qquad f(r) = -ce^{-ar^2}(1 - br^2)$$

$V_{\mathrm{low-k}}$: the configurations of $V_{NN}(k, k')$ are restricted to those with $k, k' < k_{\mathrm{cutoff}} = \Lambda$

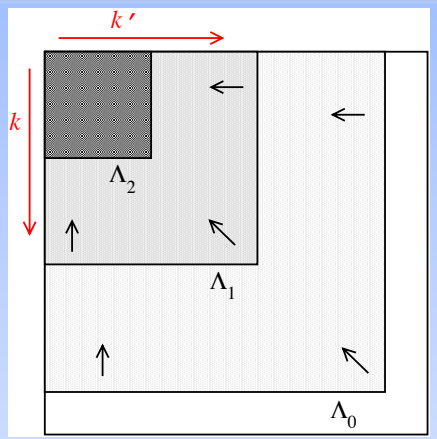

$$V_{NN}(k, k') \to V_{\mathrm{low-k}}(k, k') = \Omega^{-1} V_{NN}(k, k')\Omega$$

Consistently, we transform the $0\nu\beta\beta$ operator by way of the same similarity transformation Ω

$$\Theta(k, k') \to \Theta_{\mathrm{low-k}}(k, k') = \Omega^{-1}\Theta(k, k')\Omega$$

Shell model calculations of $M^{0\nu}$

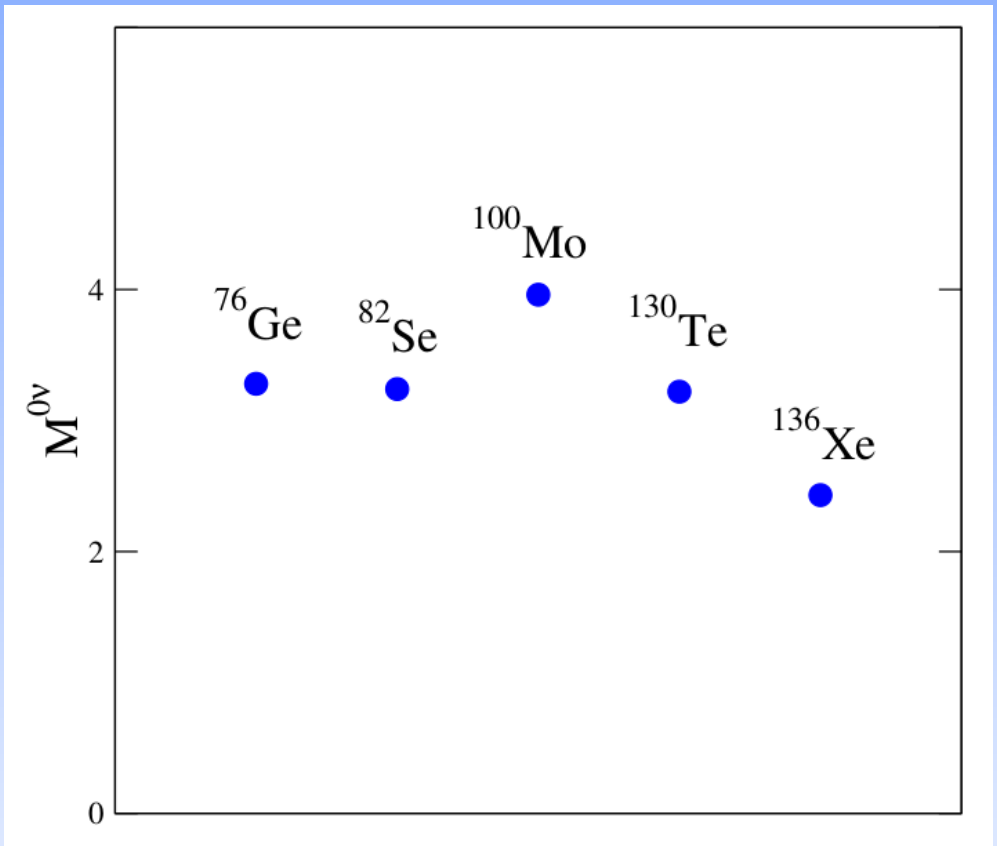

⇒ Blue dots: RSM, bare $0\nu\beta\beta$ operator

⇒ Black dots: RSM, effective $0\nu\beta\beta$ operator

Shell model calculations of $M^{0\nu}$

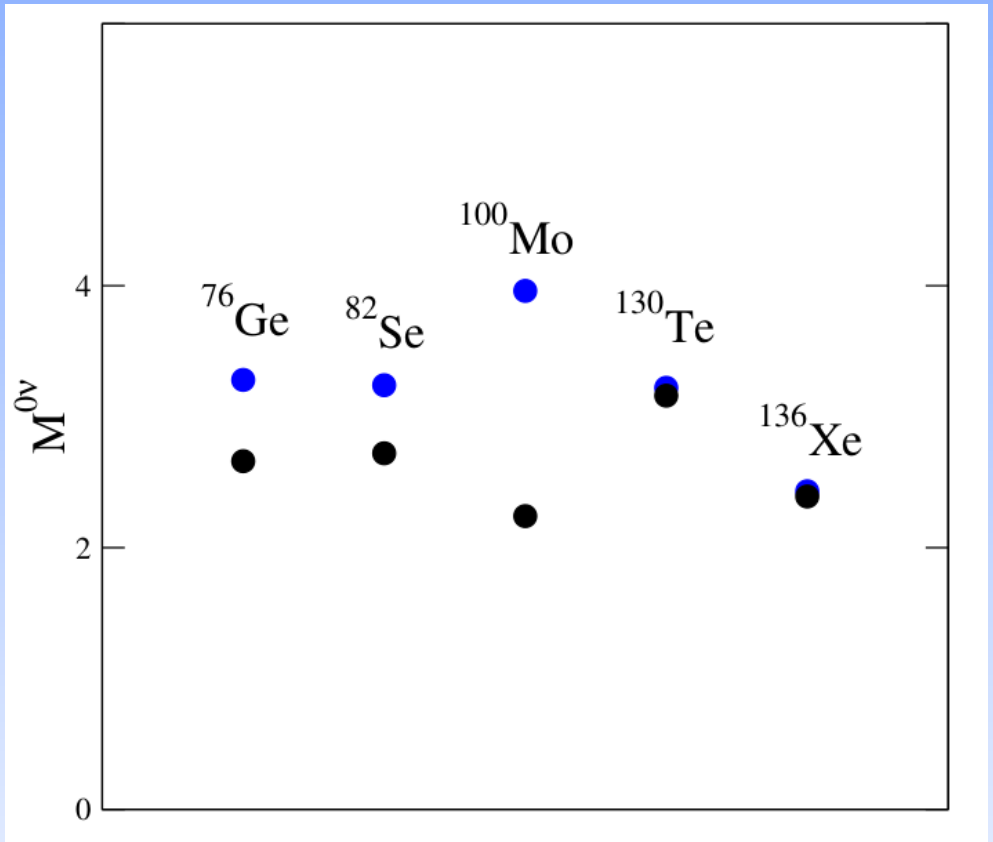

⇒ Blue dots: RSM, bare $0\nu\beta\beta$ operator

⇒ Black dots: RSM, effective $0\nu\beta\beta$ operator

Experimental upper bounds & Sensitivity

KamLAND-Zen for $^{136}\text{Xe} \rightarrow T^{0\nu}_{1/2} > 1.07 \times 10^{26}$ yr

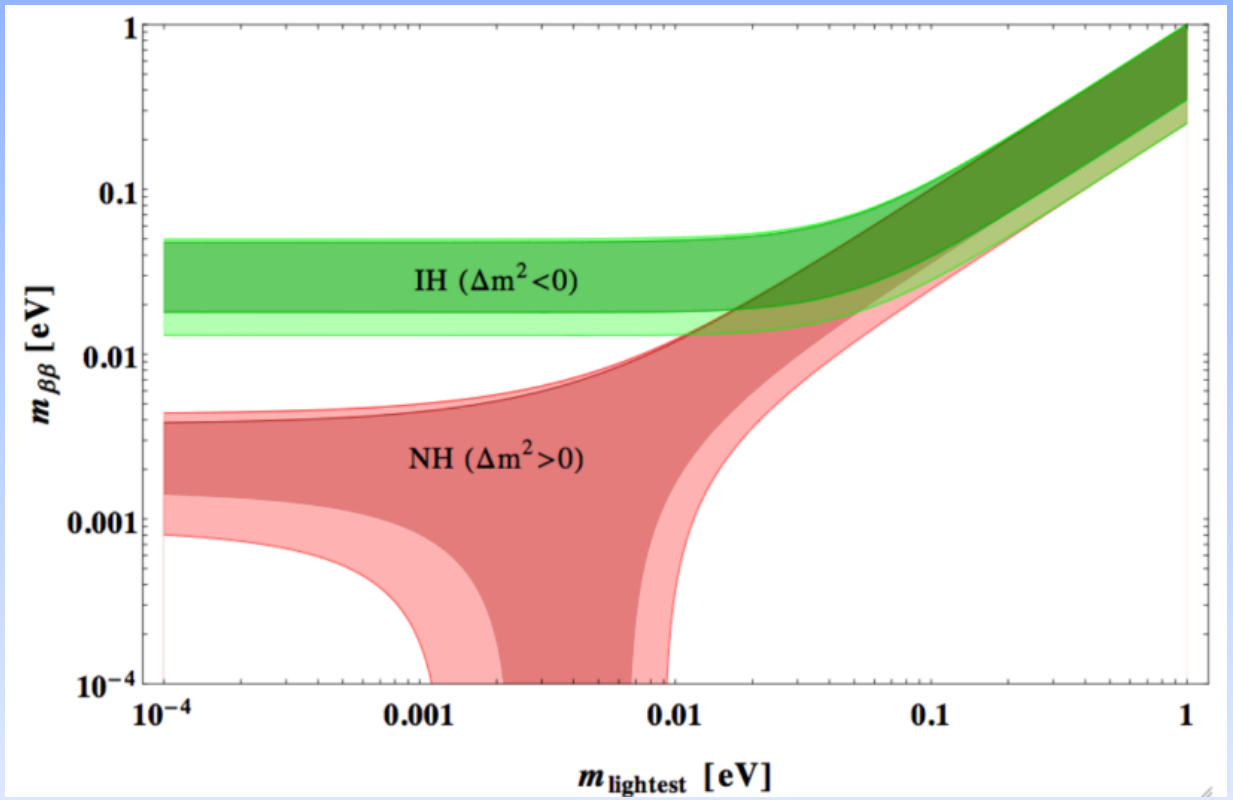

$T^{0\nu}_{1/2}$ (in yr)	$^{76}\text{Ge} \rightarrow ^{76}\text{Se}$	$^{82}\text{Se} \rightarrow ^{82}\text{Kr}$	$^{100}\text{Mo} \rightarrow ^{100}\text{Ru}$	$^{130}\text{Te} \rightarrow ^{130}\text{Xe}$	$^{136}\text{Xe} \rightarrow ^{136}\text{Ba}$
	$> 2 \times 10^{28}$	$> 4 \times 10^{27}$	$> 4 \times 10^{27}$	$> 2 \times 10^{27}$	$> 4 \times 10^{27}$

Experimental upper bounds & Sensitivity

KamLAND-Zen for $^{136}\text{Xe} \rightarrow T^{0\nu}_{1/2} > 1.07 \times 10^{26}$ yr

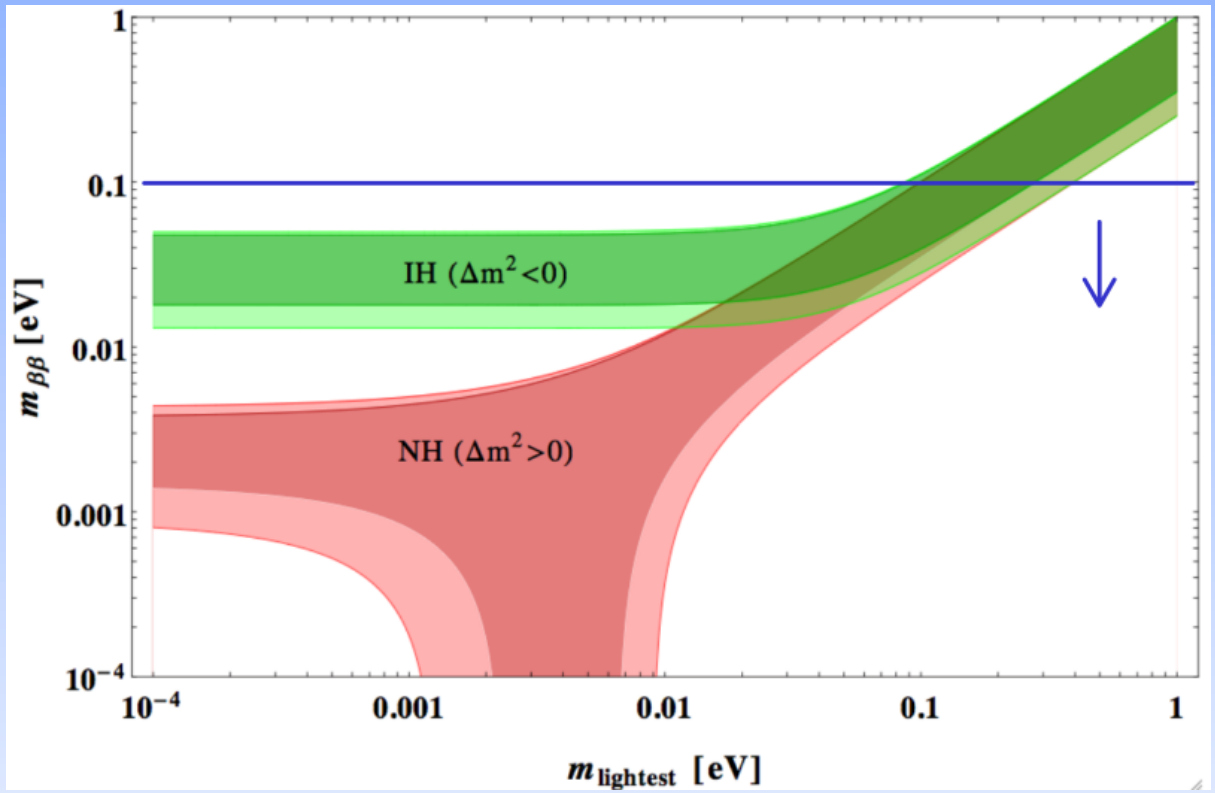

	$^{76}\text{Ge} \rightarrow ^{76}\text{Se}$	$^{82}\text{Se} \rightarrow ^{82}\text{Kr}$	$^{100}\text{Mo} \rightarrow ^{100}\text{Ru}$	$^{130}\text{Te} \rightarrow ^{130}\text{Xe}$	$^{136}\text{Xe} \rightarrow ^{136}\text{Ba}$
$T^{0\nu}_{1/2}$ (in yr)	$> 2 \times 10^{28}$	$> 4 \times 10^{27}$	$> 4 \times 10^{27}$	$> 2 \times 10^{27}$	$> 4 \times 10^{27}$

Experimental upper bounds & Sensitivity

To rule out IH $\rightarrow$ $m_{\beta\beta} < 18.4 \pm 1.3$ meV

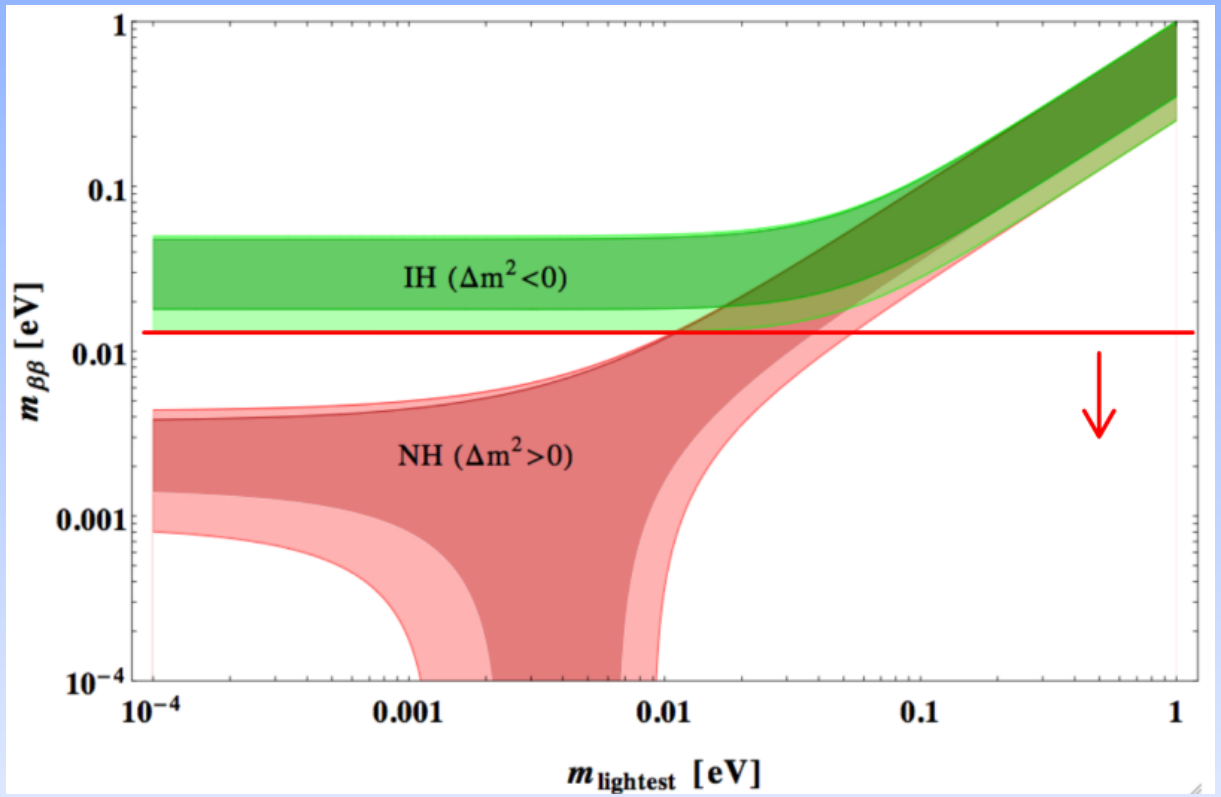

	^{76}Ge $\rightarrow$ ^{76}Se	^{82}Se $\rightarrow$ ^{82}Kr	^{100}Mo $\rightarrow$ ^{100}Ru	^{130}Te $\rightarrow$ ^{130}Xe	^{136}Xe $\rightarrow$ ^{136}Ba
$T^{0\nu}_{1/2}$ (in yr)	$> 2 \times 10^{28}$	$> 4 \times 10^{27}$	$> 4 \times 10^{27}$	$> 2 \times 10^{27}$	$> 4 \times 10^{27}$

Experimental upper bounds & Sensitivity

To rule out IH $\rightarrow$ $m_{\beta\beta} < 18.4 \pm 1.3$ meV

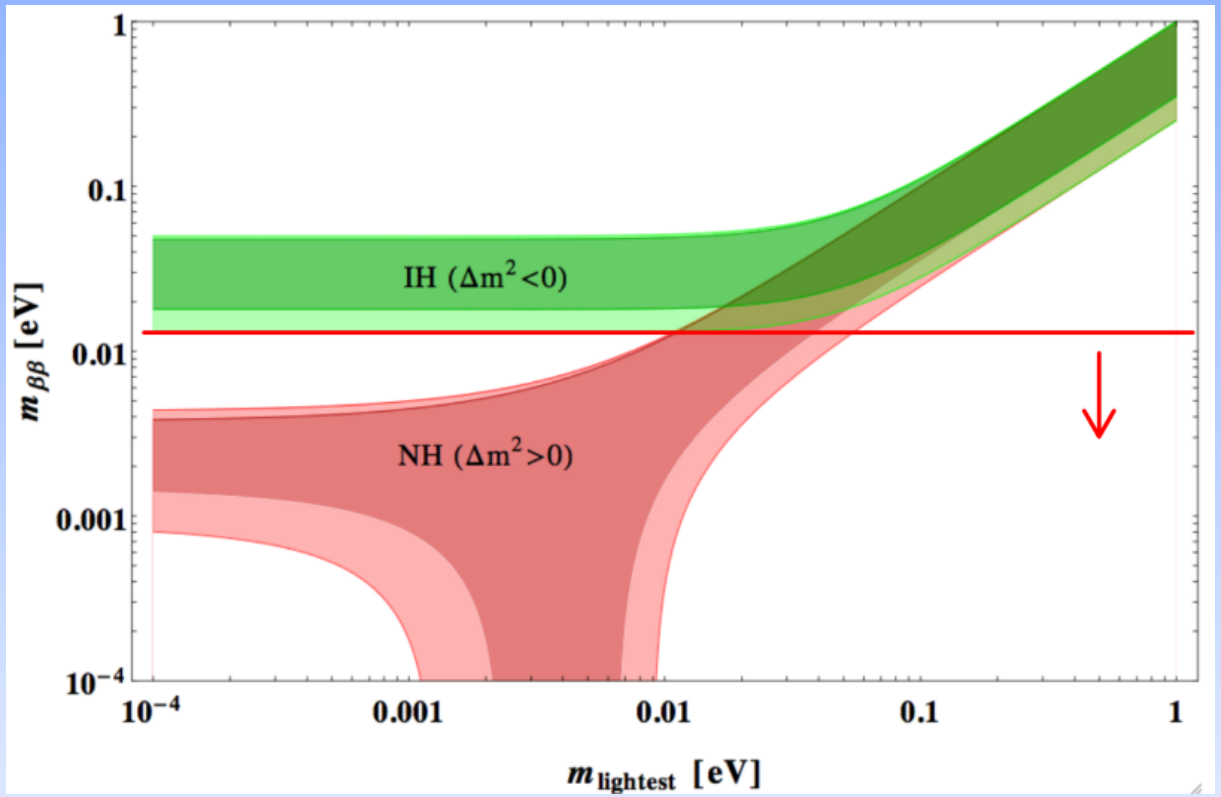

$T^{0\nu}_{1/2}$ (in yr)	^{76}Ge $\rightarrow ^{76}$ Se	^{82}Se $\rightarrow ^{82}$ Kr	^{100}Mo $\rightarrow ^{100}$ Ru	^{130}Te $\rightarrow ^{130}$ Xe	^{136}Xe $\rightarrow ^{136}$ Ba
	$> 2 \times 10^{28}$	$> 4 \times 10^{27}$	$> 4 \times 10^{27}$	$> 2 \times 10^{27}$	$> 4 \times 10^{27}$

Conclusions & Perspectives

- RSM with consistent effective GT operators $\Rightarrow$ quite good description of $\sigma\tau$ observables
- $0\nu\beta\beta$ matrix elements much less "quenched" respecto to $2\nu\beta\beta$

- Nuclear Hamiltonian and electroweak currents derived consistently by way of χPT
  - electroweak 2BC $\Rightarrow$ $\sigma\tau$ observables
  - LO contact term $\Rightarrow$ $0\nu\beta\beta$ matrix elements

Conclusions & Perspectives

- RSM with consistent effective *GT* operators $\Rightarrow$ quite good description of $\sigma\tau$ observables
- $0\nu\beta\beta$ matrix elements much less "quenched" respecto to $2\nu\beta\beta$

- Nuclear Hamiltonian and electroweak currents derived consistently by way of χPT
  - electroweak 2BC $\Rightarrow$ $\sigma\tau$ observables
  - LO contact term $\Rightarrow$ $0\nu\beta\beta$ matrix elements

Two-body electroweak currents

- EFT provides a powerful approach where both nuclear potentials and two-body electroweak currents may be consistently constructed, the latter appearing as subleading corrections to the one-body GT operator $\sigma\tau^{\pm}$

Nuclear potential

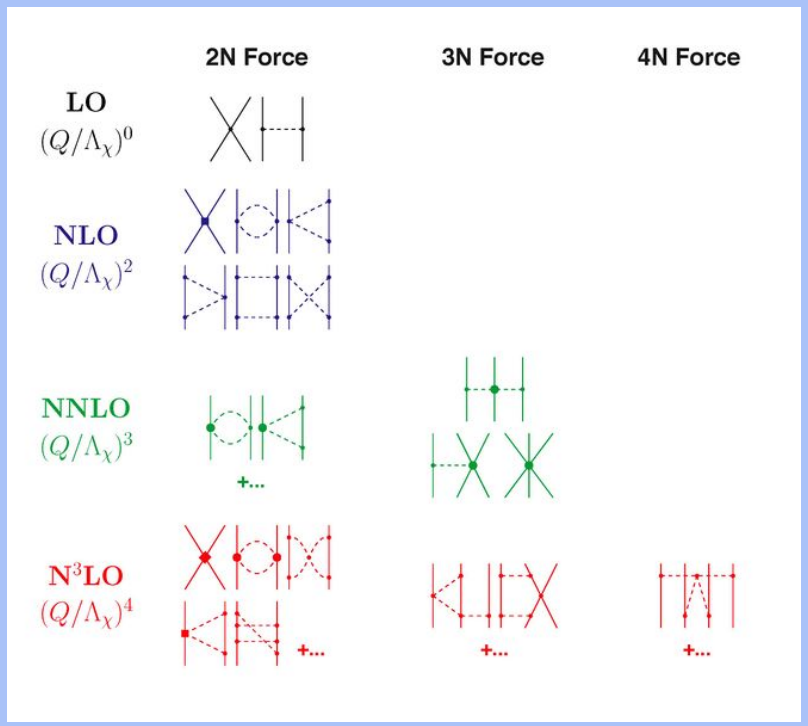

Electroweak axial currents

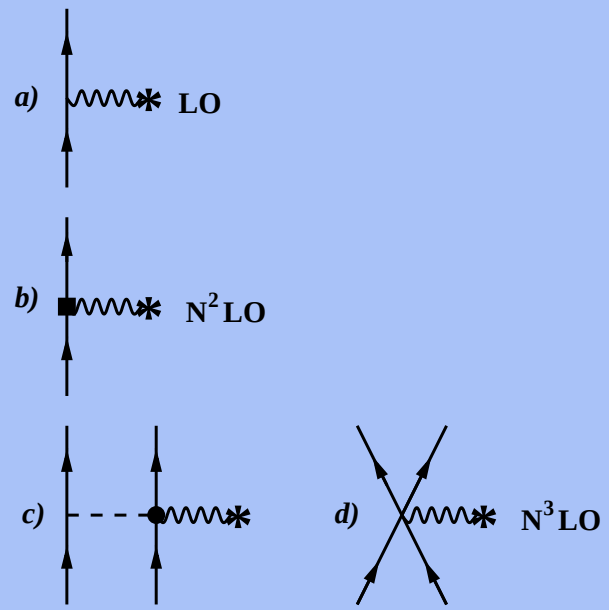

della Campania
Luigi Vanvitelli

Two-body electroweak currents

- EFT provides a powerful approach where both nuclear potentials and two-body electroweak currents may be consistently constructed, the latter appearing as subleading corrections to the one-body GT operator $\sigma\tau^{\pm}$

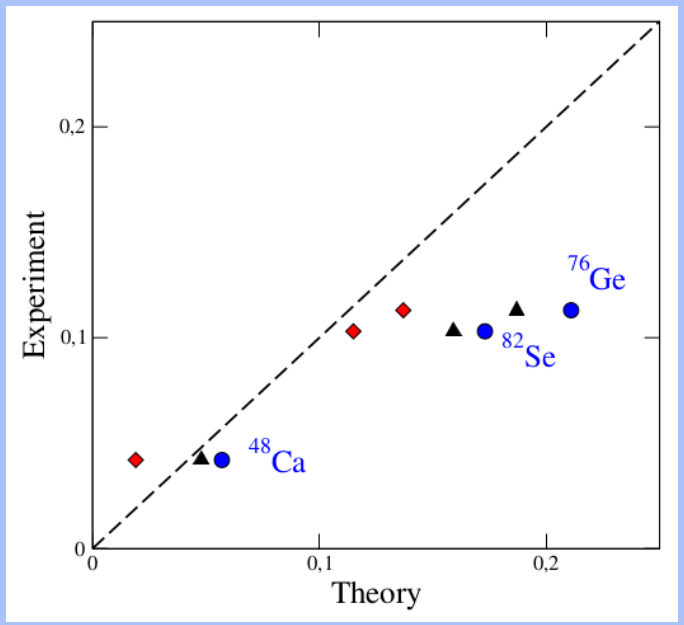

Blue dots:
bare $\mathbf{J}_A$ at LO in ChPT (namely the GT operator $g_A\sigma\cdot\tau$)

Black triangles:
effective $\mathbf{J}_A$ at LO in ChPT

Red diamonds:
effective $\mathbf{J}_A$ at N^{3}LO in ChPT

L. Coraggio, NI., G. De Gregorio, A. Gargano, Z.H. Cheng, Y.Z. Ma, F.R. Xu, and M. Viviani, accepted for publication in Phys. Rev. C

The calculation of $M^{0\nu}$: LO contact transition operator

Within the framework of χEFT, there is the need to introduce a LO short-range operator, which is missing in standard calculations of $M^{0\nu}$, to renormalize the operator and to make it independent on the ultraviolet regulator

V. Cirigliano et al., Phys. Rev. Lett. **120** *202001 (2020)*

$$M^{0\nu}_{sr} = \frac{1.2A^{1/3}\,\mathrm{fm}}{g_A^2}\langle 0^+_f|\sum_{n,m}\tau^-_m\tau^-_n\,\mathbf{1}\left[\frac{4g^{\mathrm{NN}}_\nu}{\pi}\int j_0(qr)\,f_S(p/\Lambda_S)\,q^2dq\right]|0^+_i\rangle$$

The key question is the determination of the low-energy constant g^{NN}_ν